Supplementary Information

Solvent-Free Confinement of Ordered Microparticle Monolayers: Effect of host substrate and pattern symmetry

Ignaas S. M. Jimidar,[*,†,‡] Mitch de Waard,[†,‡] Gijs Roozendaal,[¶,‡] and Kai Sotthewes[*,¶]

†*Department of Chemical Engineering CHIS, Vrije Universiteit Brussel, Brussels, 1050, Belgium*

‡*Mesoscale Chemical Systems, MESA+ Institute, University of Twente, P.O. Box 217, 7500AE Enschede, The Netherlands*

¶*Physics of Interfaces and Nanomaterials, MESA+ Institute, University of Twente, P.O. Box 217, 7500AE Enschede, The Netherlands*

E-mail: ignaas.jimidar@vub.be;i.s.m.jimidar@utwente.nl; k.sotthewes@utwente.nl

Contents

1 Detection

A MATLAB script was implemented to detect the spheres, extracting their centre coordinates and corresponding radii. Based on the size and geometry of the patterns (e.g., square, circle), a region of interest (ROI) is overlaid on the optical image, accurately reflecting the dimensions and shape of each figure. The ROI is then manually aligned with the particle-covered pattern. This ensures that, despite any crystal formation outside the CF_x pattern, the analyzed area remains consistent for all figures with the same size and shape.

A circular Hough transform was applied in MATLAB to iteratively determine the appropriate pixel range for detecting sphere radii. Additionally, a sensitivity factor was introduced to fine-tune the detection threshold. Typically, higher sensitivity allows for detecting more circular objects, including faint or partially obscured circles. In cases where patterns are imaged near the edges of the microscope's field of view, a higher sensitivity factor (≥ 0.985) is often required, particularly for larger geometries.

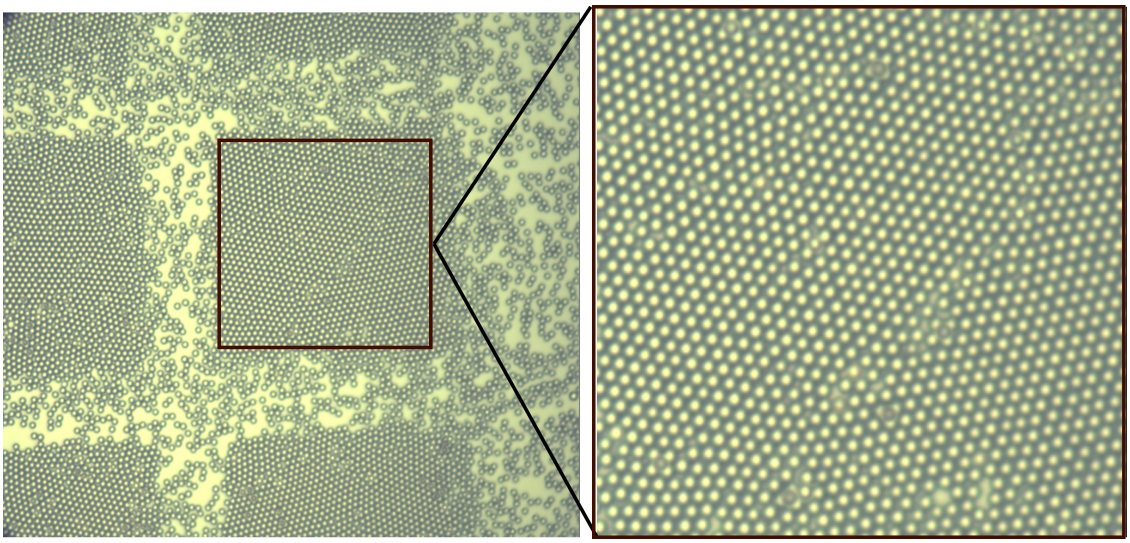

Figure S1: Image showing the ROI that is exported for image analysis.

2 Shape factor data

The shape factor data was used to derive an overall metric for the packing quality of the assembled monolayers. Voronoi diagrams were used to construct the packing arrangement. The shape factor of each individual Voronoi cell was normalized to that of an ideally regular hexagonal cell, $\vartheta = 1.1027$, such that the normalized shape factor for a hexagon becomes $\vartheta_{\text{norm,hex}} = 1$. The shape factor data was generated for each CF_x square. Since no hexagonal cells can be formed at the edge as the particle can not have six neighbours, no accurate $\vartheta_{\text{norm,hex}}$ can be computed at these locations, resulting in significantly high shape factors. To minimize the influence of these edge effects, a cut-off value for $\vartheta_{\text{norm,hex}}$ was set, excluding Voronoi cells with $\vartheta_{\text{norm,hex}} \geq 1.5$ from the dataset. Ideally, a lower cut-off would be preferred to reduce edge effects further. However, since $\vartheta \geq 1.5$ values also appear within the bulk of the figures due to various types of (symmetry) defects, it is only fair to take a value incorporating these defects in the analysis.

3 Grain identifications

The various grains assembled with the attained HCP-ordered monolayers can be identified using a composed routine. This starts by using the ROI image, as obtained by 1, see Figure S1 (right). Figure S2 presents an overview of the entire routine. The local bond order was also mapped onto the Voronoi diagram. This order parameter reflects the six-fold symmetry around a sphere. In the case of a hexagonally close-packed structure with six neighbouring spheres, the local bond orientational order is given by:

$$\Psi_6(i) = \frac{1}{N_b(i)} \sum_{j=1}^{N_b(i)} e^{i6\theta_{ij}} \tag{S1}$$

In which Ψ_6 represents the length of the net vector of the respective particle inside the six-fold lattice. As such, in the perfectly symmetric case where all particles are equidistant from

the central sphere, $\Psi_6 = 1$. Likewise, each particle contains a phase angle (θ), which shows the net orientation of the particle within the lattice.

For the detection of grains, based on the bond order plot (Figure S2C) and phase angle plot (Figure S2D), several criteria are established in which groups of particles can belong to a specific grain. It's important to note that although variations in the phase angle between neighbouring particles within a grain must remain below a certain threshold value, θ_{ij} the local orientation within the packing can vary over long distances. This is typical in two-dimensional crystals and has been previously addressed by Gray et al.[1] In previous work on 2D colloidal packing, a criterion was derived in which each respective particle has at least three adjacent neighbours, who also satisfy the criteria for Ψ_6 and θ_{ij}.[2]

To account for longer distance testing, a Breadth-First Search (BFS) algorithm[3] was applied. This approach helps identify grains. Starting with unprocessed particles whose bond order exceeded a threshold, BFS explores all adjacent particles, checking if each neighbour has a similar bond order and if the angular difference between particles is below a defined threshold. Particles meeting these criteria are assigned the same grain ID and are marked as processed. After randomly assigning a seed particle, the BFS algorithm continues iteratively until all connected particles are grouped. As a result of the correct parameter search, the following criteria were set:

- **Local bond orientational order:** The first step to identify grains is to incorporate only particles with a good six-fold symmetry by excluding spheres based on their bond order. By plotting a Voronoi diagram with individual ψ_6 values, as shown in Figure S2(C), disruptions in the perfectly ordered HCP packing are noted. This is observed by the blue or green-coloured cells, clearly indicating the boundaries of a grain. Accordingly, Voronoi cells with Ψ_6 as high as 0.85 still show hexagonal symmetry, albeit imperfect, which can also be attributed to detection limits. As such, a minimum cut-off value of $\psi_6 \geq 0.85$ was set.

- **Phase angle** (θ): As shown by the encircled region of Figure S2D, transitions can be

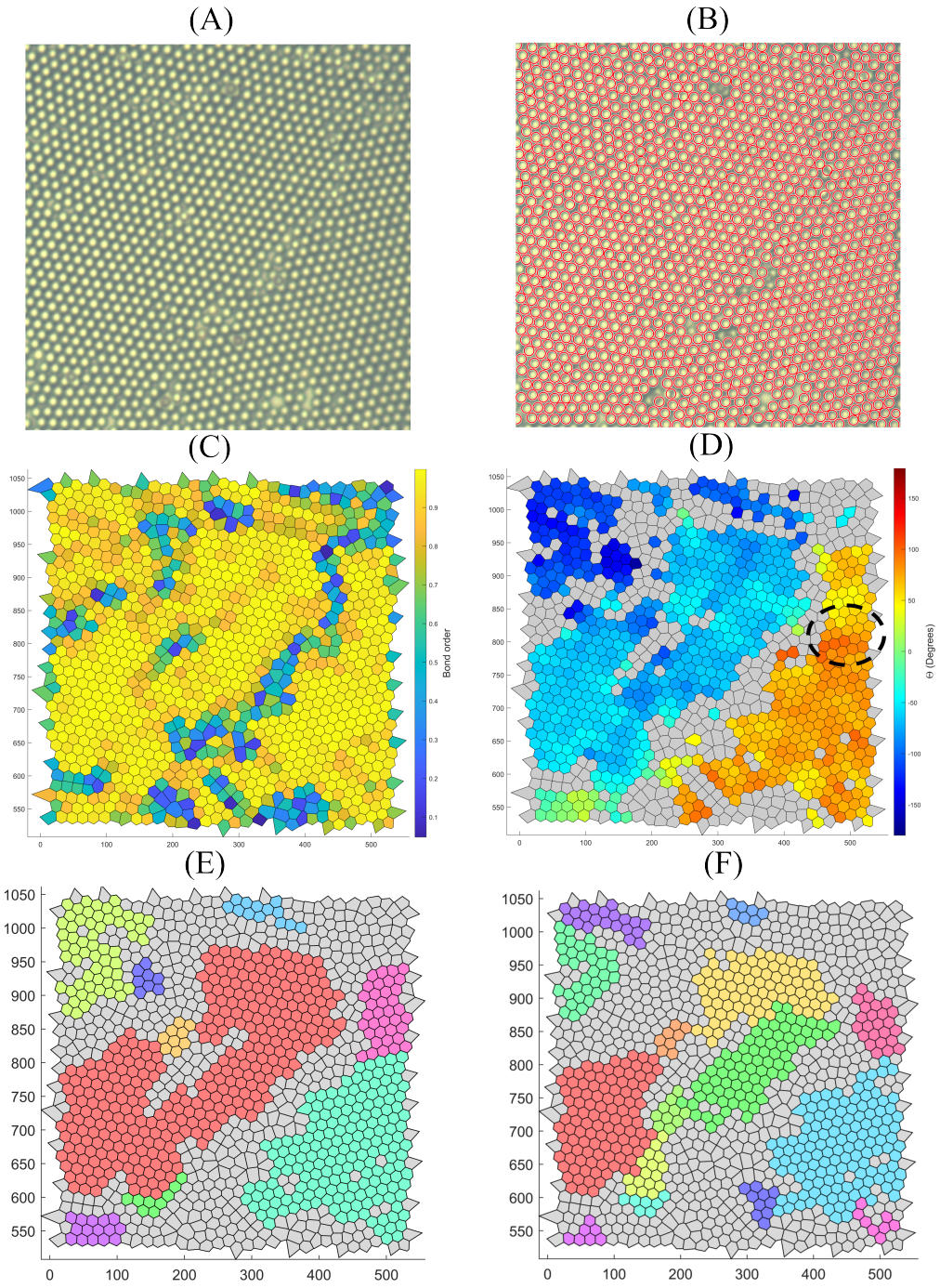

Figure S2: Workflow for grain computation, in consecutive order from A-E. (A) The cropped ROI image, as sliced from the raw Microscope image. (B) Overlay image of the detected particles following circle recognition. (C) Voronoi tessellation image, showing the values of the local bond orientational number, Ψ_6. (D) Phase angle plot after filtering out $\Psi_6 \leq 0.85$. Note the encircled region that clearly shows a sudden change in orientation. (E) Computation of grains for $\theta_{ij} = 10°$, used for all analyzed figures. (F) Computation of grains for $\theta_{ij} = 7°$, which was found too strict for the analyzed figures.

identified in which there is a clear shift in phase angle. By manually checking whether these regions can be identified as distinct grains, θ_{ij} was eventually set to 10°.

- **Minimal amount of particles per grain:** Grains with less than 7 particles are discarded, i.e., not counted as a grain, as we have defined a minimum number of an HCP crystal unit cell comprising at least 7 particles.

This approach ensures that grains are formed based on both spatial proximity (neighbours) and similarity in their rotational symmetry (phase magnitude and angle).

4 Nearest neighbor edge count

Since the geometrical shape of the confined CF_x patterns, i.e. the effect of edges, is expected to affect the formation of grains, the following part of the analysis is used to characterize the particle order near the edges. For each geometry, the edges were defined by specifying the coordinates of the corners. Subsequently, a nearest neighbour function was applied, considering the distance between the particles in a close packing arrangement. Several criteria have been applied to retrieve a dataset containing particles only near the edges, i.e.

- **Nearest neighbour distance:** To consider a particle as a near neighbour, a minimum distance between the centre of circles is adopted. As such, the centre-to-centre distance between neighbouring particles of $D_p = 3$ µm is 18 pixels. The plot was manually examined to validate the correct distance length, resulting in a slightly larger distance measure of 19 pixels. This indicates that particles within such distance of the respective particle can be classified as one of their nearest neighbours.

- **Number of Nearest neighbour :** Near the edge of the figure, it should be noted that particles can contain somewhere between 0 and 4 nearest neighbours. As such, particles with NN > 4 should solely be found in the bulk of the figures and should thus be excluded.

- **Edge margin:** The edge margin refers to the distance from the edge of a figure within which the centre of a particle can be placed, assigning it to the outermost layer of particles that make up the figure. As such, it has been detected by using the ROI coordinates, as obtained by Section 1. For a square figure, this means the size of the cropped image, whereas, in the case of a circle, the ROI is defined by its centre and respective radius. From the edge of the ROI, an optimum distance X_i was iteratively found, in which the second layer of the shell would be excluded whilst making sure that the centres of the outer layer would be included to characterize the order at the edge between the CF_x square and the host substrates.

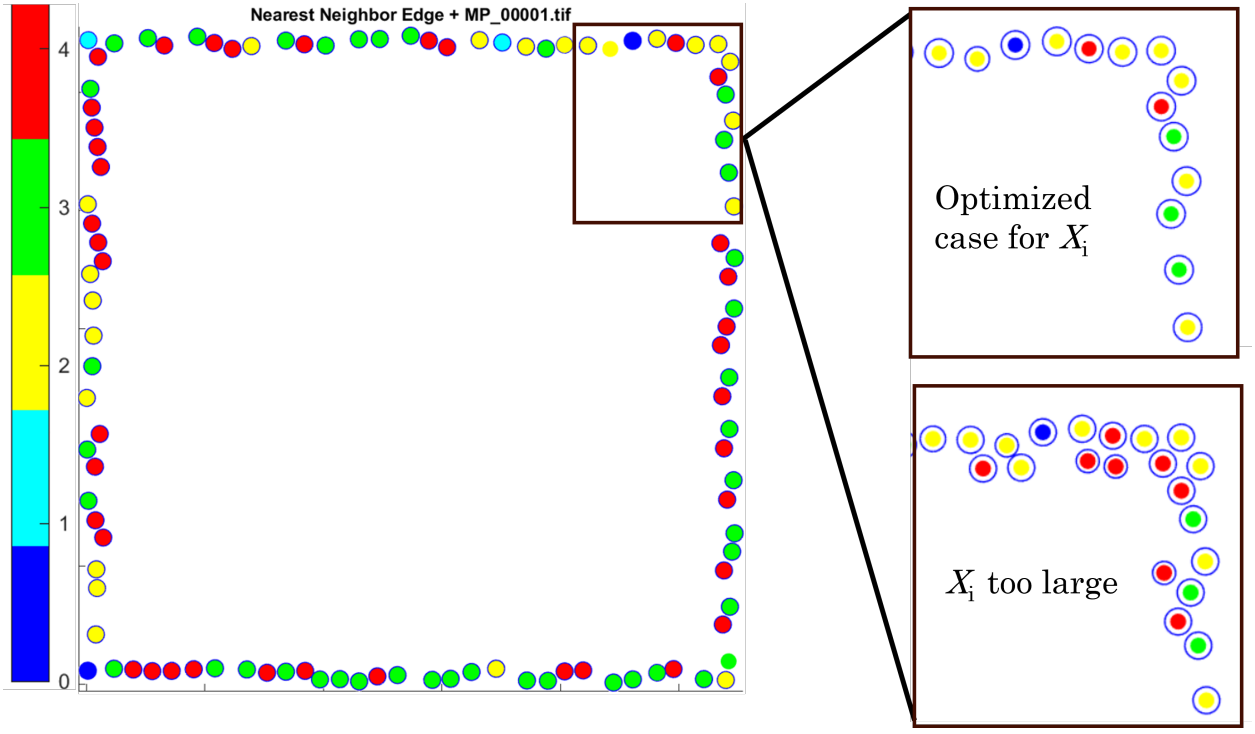

Figure S3: Effect of X_i on the detection of edge particles.

5 Additional data

Fig. S4 shows the nearest neighbour distribution for circle, square and triangular patterns with form factors 11 (Fig. S4(A)) and 25 (Fig. S4(B)). Similar results are obtained as shown in Fig. 4(B) of the main text.

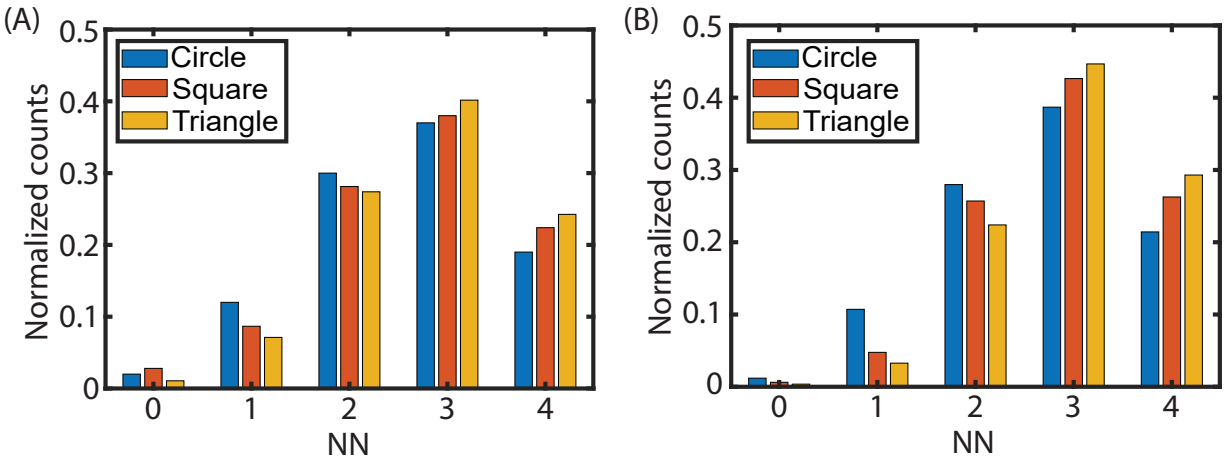

Figure S4: (A-B) Distribution of the number of nearest neighbours (NN) of 3 μm PMMA edge particles (particles located at the edge) on patterns with different geometrical shapes. The form factors (FF) of the different shapes is approximately 11 in (A) and 25 in (B).

Fig. S5 shows the average number of particles per grain as a function of the square pattern size. Similar to the coverage (Fig. 2(C) of the main text), the number of particles per grain is much higher when SiO_2 is used as a host substrate. The larger number of particles per grain is also reflected in the lower average number of grains present on the patterns (Fig. 2(B) of the main text).

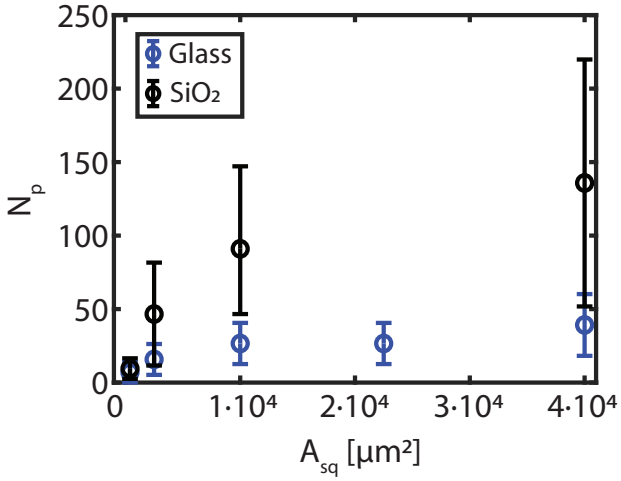

Figure S5: The average number of microparticles (N_{P}) per grain for different square pattern areas.

References

(1) Gray, A.; Mould, E.; Royall, C.; Williams, I. Structural characterisation of polycrystalline colloidal monolayers in the presence of aspherical impurities. *Journal of physics. Condensed matter : an Institute of Physics journal* **2015**, *27*.

(2) Dillmann, P.; Maret, G.; Keim, P. Polycrystalline solidification in a quenched 2D colloidal system. *Journal of Physics: Condensed Matter* **2008**, *20*, 404216.

(3) Silvela, J.; Portillo, J. Breadth-first search and its application to image processing problems. *IEEE Transactions on Image Processing* **2001**, *10*, 1194–1199.